

# BOW SHOCKS AROUND PULSARS AND NEUTRON STARS

Bryan M. Gaensler

*Harvard-Smithsonian Center for Astrophysics, 60 Garden Street MS-6,  
Cambridge, MA 02138, USA*

---

## Abstract

Pulsar wind nebulae are now well established as important probes both of neutron stars' relativistic winds and of the surrounding interstellar medium. Amongst this diverse group of objects, pulsar bow shocks have long been regarded as an oddity, only seen around a handful of rapidly moving neutron stars. However, recent efforts at optical, radio and X-ray wavelengths have identified many new pulsar bow shocks, and these results have consequently motivated renewed theoretical efforts to model these systems. Here I review the new results and ideas which have emerged on these spectacular systems, and explain how bow shocks and “Crab-like” nebulae now form a consistent picture within our understanding of pulsar winds.

*Key words:*

ISM: general, stars: neutron, stars: winds, outflows

---

## 1 Introduction

Pulsars have high space velocities, typically in the range 150–1500 km s<sup>-1</sup> (Arzoumanian, Chernoff, and Cordes, 2002). Since such speeds are well in excess of typical sound speeds for the cold ( $\sim 1$  km s<sup>-1</sup>) or warm components ( $\sim 10$  km s<sup>-1</sup>) of the interstellar medium (ISM), we expect that many pulsars are moving supersonically, and that they should thus drive bow shocks through ambient gas.

Such phenomena are, of course, not unique: astrophysical bow shocks are seen around proto-stars, clumps of supernova ejecta, runaway OB stars, and in the solar wind (e.g., Kaper et al., 1997; van Buren and McCray, 1988; Sutherland and Dopita, 1995; Zank, 1999). However, several factors make pulsar bow shocks particularly appealing to study. First, for pulsars the mechanical luminosity of the wind driving the bow shock can be reasonably estimated through the pulsar's

“spin-down luminosity”, given by  $\dot{E} \equiv 4\pi^2 I \dot{P} / P^3$  (where  $I \equiv 10^{45}$  g cm<sup>2</sup> is the neutron star’s assumed moment of inertia,  $P$  is the star’s spin period, and  $\dot{P}$  is the period derivative). Spin-down luminosities for observed pulsars are typically in the range  $10^{32} - 10^{39}$  ergs s<sup>-1</sup>. Second, for many pulsars, precision timing and interferometric measurements allow accurate determinations of the star’s position and proper motion. Finally, compared to many other Galactic populations, the distances to pulsars are reasonably well-established — from parallax for about 20 sources (e.g., Chatterjee et al., 2004), and from dispersion of the pulsed radio signals for over 1500 others (Cordes and Lazio, 2002). All these factors mean that many of the unknowns generally associated with bow shocks are not an issue for pulsars; in principle, the only parameters to be determined are the density and structure of the ISM, plus the inclination angle of the system.

Furthermore, most pulsars are  $10^6 - 10^9$  years old, their high space velocities having carried them far from their birth places. This means that pulsars are more or less randomly located within the Galactic disk, and that their bow shocks can thus act as unbiased probes of the ISM. Bow shocks also potentially provide an opportunity to study the winds of “typical” pulsars, rather than extreme cases of youth and energy as typified by the Crab Nebula.

Despite their potential as useful probes of pulsars and their surroundings, very few pulsar bow shocks were known until recently. Because of several recent discoveries and accompanying theoretical modelling, there has been renewed interest in these systems in the last few years. Here I summarise recent work, and the resulting improvements to our understanding. For earlier reviews on bow shocks see Cordes (1996) and Chatterjee and Cordes (2002); for more general discussion of pulsar wind nebulae, the reader is referred to reviews by Gaensler (2004) and Kaspi et al. (2005).

## 2 Theoretical Expectations

Several authors have considered the theory of bow shocks in detail, both under general circumstances (Chen et al., 1996; Wilkin, 1996, 2000) and specifically in the case of pulsars (Aldcroft et al., 1992; Bucciantini, 2002a,b; van der Swaluw et al., 2003). Some pertinent points from these studies are as follows.

**Scaling Parameter:** One parameter sets the overall scale of a bow shock — the “stand-off distance”,  $r_w$ . This is the separation between the pulsar position and the apex of the bow shock, and is set by pressure balance,

$$\frac{\dot{E}}{4\pi r_w^2 c} = \rho V^2, \tag{1}$$

Fig. 1. Hydrodynamic simulation of a pulsar bow shock, adapted from Bucciantini (2002a). The greyscale indicates density; the pulsar is moving from right to left with a Mach number  $\mathcal{M} \sim 13$ . Various regions and interfaces discussed in the text are indicated.

where  $\rho$  is the ambient mass density and  $V$  is the pulsar’s space velocity relative to its surroundings.

**Shape:** Wilkin (1996) has provided an elegant analytic solution to the shape of a bow shock,

$$r(\theta) = r_w \csc \theta \sqrt{3(1 - \theta \cot \theta)}, \quad (2)$$

where  $r(\theta)$  is the radius of the bow shock at a polar angle  $\theta$ . This solution is for an idealised thin-layer shock, but is also expected to be a reasonable approximation to pulsar bow shocks in regions near the apex (Bucciantini, 2002a; van der Swaluw et al., 2003).

**Overall Structure:** Because of the long cooling time scales, bow shocks are not thin shells, but show a characteristic double-shock structure, as shown in Figure 1. The morphology consists of a forward shock which heats the ISM, a termination shock which decelerates the pulsar wind, and a contact discontinuity dividing shocked ISM from shocked pulsar wind material.

**Termination Shock:** The pulsar wind experiences a significant difference in pressure between regions ahead of and behind the pulsar’s motion. The termination shock is therefore not of uniform radius around the pulsar, but rather has a bullet-shaped morphology, the head of the bullet aligned with the pulsar’s direction of motion as can be seen in Figure 1. For low Mach numbers,  $\mathcal{M} \sim 1$ , the ratio of termination shock radii between the directions immediately behind and directly ahead of the pulsar is roughly proportional to  $\mathcal{M}$  (Bucciantini, 2002a; van der Swaluw et al., 2003). However, in the limit of high Mach number, this ratio tends to an asymptotic limit of about 5

(Gaensler et al., 2004).

### 3 Observations: Forward Shock

The forward shock should produce observable  $H\alpha$  emission, resulting from collisional excitation and charge exchange of neutrals in ambient gas. Indeed some beautiful bow shocks have been observed in the  $H\alpha$  line, several of which have been discovered just in the last few years (van Kerkwijk and Kulkarni, 2001; Jones et al., 2002; Gaensler et al., 2002). Detection of such a bow shock allows one to estimate measure  $r_w$ , although two cautions must be issued. First,  $r_w$  formally corresponds to the distance from the pulsar to the termination shock, not to the forward shock (e.g., Bucciantini, 2002a). So the observed pulsar/shock separation needs to be scaled by some factor, which simulations suggest has a value  $\sim 0.4 - 0.6$  (Bucciantini, 2002a; van der Swaluw et al., 2003). Second, the measured separation needs to be corrected for the (usually unknown) inclination. This correction is not a simple trigonometric factor, because projection of the three-dimensional bow-shock surface onto the sky can be larger than the true separation (Gaensler et al., 2002). Correction for inclination is non-trivial, and quantities inferred from the observed bow-shock separation should thus be considered approximate.

With these caveats in mind, pressure balance can be applied to a system in which  $\dot{E}$  and  $V$  are known to yield  $\rho$  via Equation (1). This approach suggests ambient densities  $\sim 0.1 \text{ cm}^{-3}$ , as expected for warm neutral gas in the ISM (Chatterjee and Cordes, 2002; Gaensler et al., 2002). In cases where  $V$  is not known, one can write  $\rho V^2 = \gamma \mathcal{M}^2 \mathcal{P}$ , where  $\gamma = 5/3$  is the adiabatic coefficient of the ISM and  $\mathcal{P}$  is the ISM pressure. Adoption of a typical value for  $\mathcal{P}$  allows one to directly estimate  $\mathcal{M}$ .

In the case of an isotropic pulsar wind propagating through a homogeneous ISM, Equation (2) should describe the  $H\alpha$  brightness profile well. For PSR J0437–4715 this indeed seems to be the case, allowing one to solve for the inclination angle of the system (Mann et al., 1999). However, in several other cases there are significant deviations from this idealised solution, in the form of abrupt kinks and bulges in the bow-shock profile, or a rotational offset between the symmetry axis of the bow shock and the velocity vector of the pulsar (e.g., PSR B0740–28, Jones et al. 2002; PSR J2124–3358, Gaensler et al. 2002). These shapes imply some combination of anisotropies in the pulsar wind (as are known to exist around young pulsars; see Gaensler 2004), density variations in the ISM, or significant motion of ambient gas with respect to the local rest-frame. Multi-epoch observations, showing changes in the bow-shock structure with time, are beginning to explore these possibilities (Chatterjee and Cordes, 2004).

## 4 Observations: Termination Shock

### 4.1 *The Mouse*

Just as is the case for younger systems like the Crab Nebula, we expect that the particles in the pulsar wind will be accelerated at the termination shock, generating radio and X-ray synchrotron emission. Indeed cometary radio and X-ray emission aligned with the direction of motion is seen around several high velocity pulsars (Chatterjee and Cordes, 2002).

Figure 2 shows the results of a recent detailed study of “the Mouse”, an elongated radio and X-ray nebula coincident with the energetic pulsar J1747–2958 (Camilo et al., 2002; Gaensler et al., 2004). The Mouse is very luminous, and thus represents an ideal opportunity to test the theories developed for bow-shock termination shocks.

If the X-ray and radio emission from the Mouse comes from the termination shock region, we expect it to be sharply bounded at its apex by the contact discontinuity. The extent of emission thus allows us to estimate the stand-off distance for this system — for a distance of 5 kpc we find  $r_w \approx 0.02$  pc. For ISM pressures  $\mathcal{P}/k = 2400P_0$  K cm<sup>-3</sup> (with typical observed values in the range  $0.5 \lesssim P_0 \lesssim 5$ ), this implies a high Mach number,  $\mathcal{M} \sim 60P_0^{-1/2}$ , and thus a likely space velocity  $V \approx 600P_0^{-1/2}$  km s<sup>-1</sup> if propagating through the warm component of the ISM.

The X-ray and radio morphologies shown in Figure 2 both indicate the presence of an elongated bright “tongue” of emission behind the pulsar, about 0.25 pc in length. An interpretation of this feature is suggested by comparison with the hydrodynamic simulation shown in Figure 1, where it can be seen that the tongue has a similar appearance to the surface of the bullet-shaped termination shock. If we make this identification, then the tongue in the Mouse is directly analogous to the inner toroidal ring seen for the Crab Nebula and other related systems (e.g., Ng and Romani, 2004), demarcating the point where the pulsar wind reacts to its surroundings and where wind particles are accelerated up to synchrotron-emitting energies.

It is important to note that hydrodynamic simulations such as that shown in Figure 1 do not explicitly include the effects of magnetic fields or relativistic flows, so an exact correspondence between the data and the model is not expected. In particular, two important discrepancies can be identified: the ratio of backward and forward termination shocks is observed to be  $\sim 10$ , rather than the value of 5 predicted for  $\mathcal{M} \gg 1$ ; and the sheath does not show any limb-brightening as would be expected given its geometry. The first of

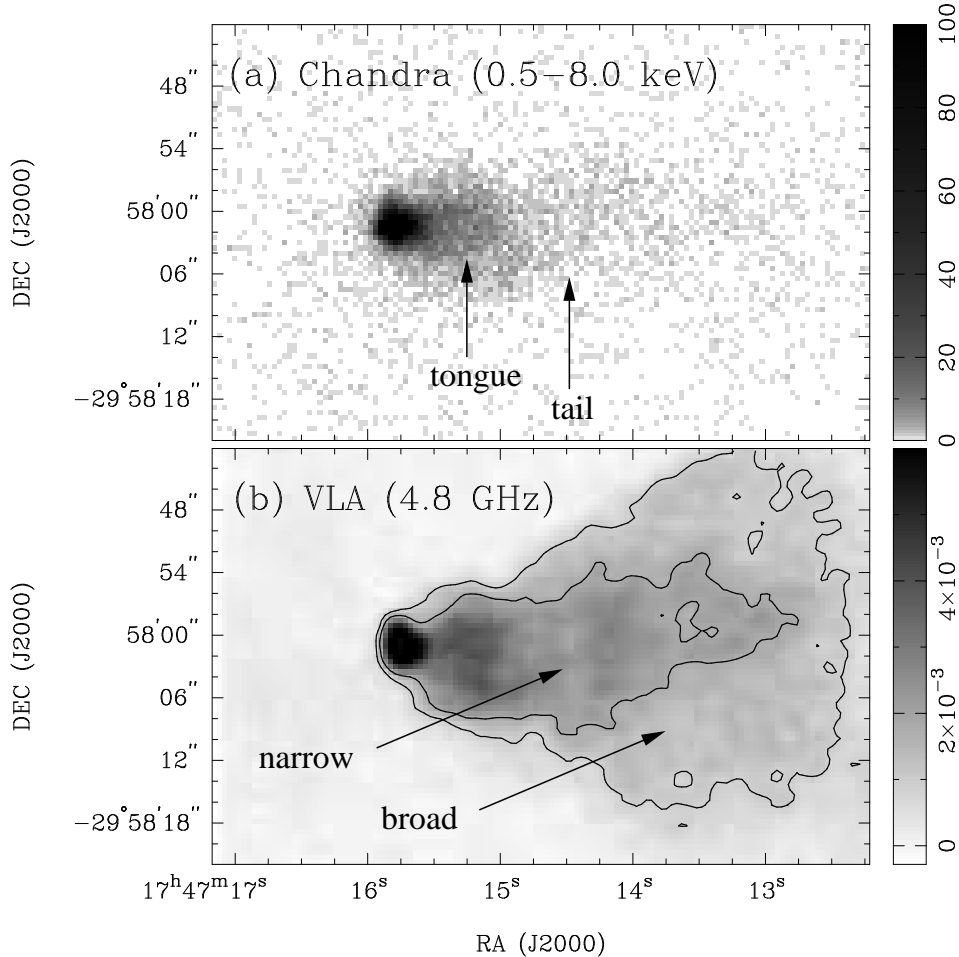


Fig. 2. X-ray (upper) and radio (lower) images of the bow shock G359.23–0.82 (a.k.a. “the Mouse”) powered by PSR J1747–2958 (Gaensler et al., 2004). In the X-ray image, the “tongue” and “tail” regions are indicated. In the radio image, the broad and narrow components of the tail are shown.

these points can potentially be explained by the effect of ions in the wind, whose gyrations in the magnetic field spread the electron shock over a large distance (Gallant and Arons, 1994). This effect should operate in the backward flow from the pulsar, but not in the forward direction due to the high degree of pressure confinement. The lack of limb brightening can be accounted for by Doppler boosting in the post-shock flow, as is consistently observed in the winds of younger, lower velocity pulsars (Ng and Romani, 2004). While confirmation of these effects will require a fully relativistic magnetohydrodynamic treatment, we emphasise that both the effects claimed here have been seen in the wind nebulae around “Crab-like” pulsars. The need to invoke similar phenomena here suggests a high degree of commonality between the wind properties of the youngest pulsars and more typical members of the population.

West of the tongue, a fading tail of emission is seen, which must come from

material significantly downstream of the termination shock. This emission is analogous to the main body of the nebula in Crab-like systems. The tail of emission behind the Mouse can be delineated into two components, as indicated in Figure 2. The first component is bright, reasonably narrow, and is seen in both radio and X-rays; the second component is broader, fainter, and is seen in radio only. These structures can be qualitatively understood by again considering the hydrodynamic simulation of Figure 1, in which it can be seen that there are two extremes in the flow. Ahead of the pulsar, the wind shocks at a small distance from the pulsar at the apex, then turns around and flows around the edges of the shocked region. In contrast, behind the pulsar the distance to the shock is considerably larger; the post-shock flow then remains in a narrow collimated region lying along the symmetry axis. If equipartition holds, so that  $\dot{E}/4\pi r_w^2 c \propto B^2$ , where  $B$  is the post-shock nebular magnetic field, then the shocked flow ahead of the pulsar should have a magnetic field  $\sim 10$  times larger than that behind the pulsar. We thus expect a broad flow in which the X-ray emission suffers severe synchrotron losses, enveloping a narrow flow in which the X-rays are yet to cool. This is in accordance with observations, suggesting that in contrast to the Crab Nebula, the pulsar’s motion structures the post-shock emitting regions into two distinct zones.

#### 4.2 *X-ray Trails Behind Other Pulsars*

Now that we have a picture of what might be occurring for the Mouse, it is insightful to consider other bow shocks which produce radio and X-ray emission, to see if similar features are observed.

Some pulsars, such as PSRs B1757–24 and B1957+20 (Kaspi et al., 2001; Stappers et al., 2003), show short ( $\sim 0.1–0.5$  pc) X-ray trails extending opposite the pulsar’s direction of motion. One interpretation is that these features are synchrotron “wakes”, i.e., particles left behind by the pulsar as it moves through the ISM. However, the time taken for a pulsar to traverse the extent of one of these trails is  $\sim 1000$  yr, implying abnormally low nebular magnetic field strengths if synchrotron cooling at X-ray energies is to be avoided during this period. It has therefore been suggested that a rapid backflow or nozzle operates downstream, which rapidly advects emitting particles and produces the trail structures observed (e.g., Wang and Gotthelf, 1998; Kaspi et al., 2001).

However, the Mouse suggests an alternative interpretation. We expect two components to the downstream synchrotron emission from a pulsar bow shock. Close to the pulsar, we should see a “tongue” of emission around the termination shock. We expect this region to show a constant X-ray spectrum across its extent, to have a comparable extent in radio and X-rays, and to abruptly terminate at a distance  $\sim 10r_w$  behind the pulsar. Further from the pulsar,

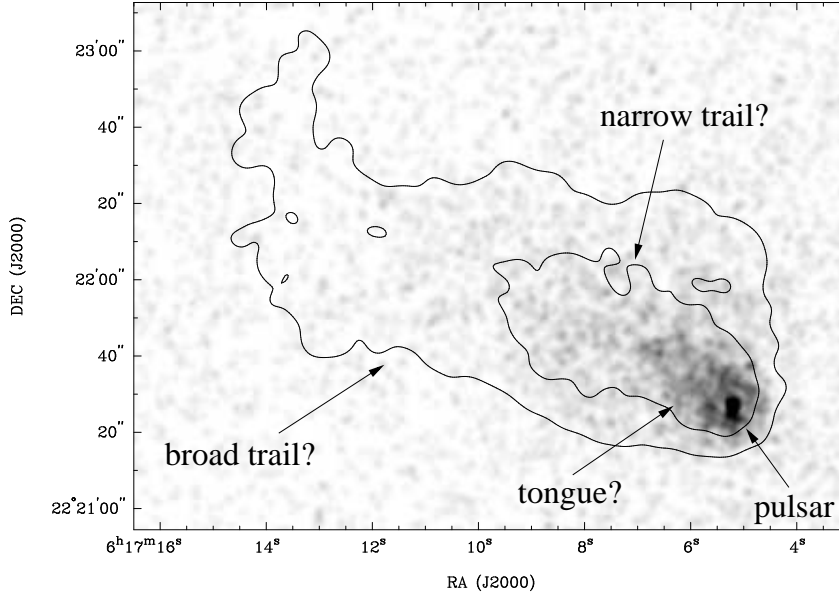


Fig. 3. X-ray and radio observations of the X-ray bow shock around CXOU J061705.3+222127 in the SNR IC 443. The image shows *Chandra* data smoothed with a  $2''$  gaussian, while contours denote 8.4-GHz VLA data at a resolution of  $7''$ . Proposed features are indicated.

the “tail” component representing post-shock material should show an X-ray spectrum which softens with distance from the pulsar, should have a larger extent in radio than in X-rays, and should gradually fade into the background over an extent  $\gg 10r_w$ .

Armed with the realisation that bow shocks should show both these components, it seems that the short trails seen around PSRs B1957+20 and B1757–24 correspond well to the tongue component of the Mouse. Gaensler et al. (2004) and Gvaramadze (2004) have thus both argued that the name “trail” is a misnomer — these features are simply the surfaces of the termination shock around these pulsars, the longer tail of emission downstream being too faint to see.

On the other hand, a closer examination of other pulsar bow shocks suggests that they too potentially show multiple components in X-rays, corresponding both to the termination shock and to the tail of emission behind it. Possible examples of such systems are PSR B1853+01 in the supernova remnant (SNR) W44 (Petre et al., 2002), PSR B1951+32 in SNR CTB 80 (Moon et al., 2004), and the neutron star CXOU J061705.3+222127 in SNR IC 443 (Olbert et al., 2001). The latter source is shown in Figure 3, where the identification of these possible structures is indicated. It is interesting to note that this source is moving through the shocked gas in the interior of an evolved SNR. In this case, we expect a Mach number  $\mathcal{M} \sim 3$  (van der Swaluw et al., 2003), much lower than for a pulsar moving through the ISM. For this low Mach number, we expect the “tongue” region to only be about half as long (in units of



$r_w$ ) than for a high Mach number system like the Mouse. Indeed the data in Figure 3 suggest an extent for this feature  $\sim 5r_w$ , compared to  $\sim 10r_w$  for the Mouse. Deeper *Chandra* observations of both CXOU J061705.3+222127 and PSR B1853+01 are scheduled to take place in 2005, which should allow a better investigation of these possibilities.

## 5 Putting It All Together

In §2, it was noted that a double-shock structure is expected around a supersonic pulsar. While we clearly see either forward or termination shocks around various neutron stars, for just one system, PSR B1957+20, have both the termination shock (in X-rays) and forward shock (in  $H\alpha$ ) been identified in the same source (Stappers et al., 2003). A collection of such sources can act as a detailed probe of the hydrodynamics of the bow-shock interaction, so expansion of this sample is obviously highly desirable.

Most of the pulsar bow shocks seen in radio/X-rays have high values of  $\dot{E}$ , meaning that they are reasonably rare and hence distant. The high extinction to these systems makes it difficult to identify any  $H\alpha$  emission around them. On the other hand,  $H\alpha$  bow shocks tend to be nearby, so are worthwhile targets for X-ray imaging, even if  $\dot{E}$  is low. But of the five other known  $H\alpha$  bow shocks besides that around PSR B1957+20, two (PSR J0437–4715, Zavlin et al. 2002; RX J1856.5–3754<sup>1</sup>) show no extended X-ray emission, one (PSR B2224+65; Wong et al. 2003) shows an X-ray filament completely misaligned with the pulsar’s direction of motion, and the remaining two (PSRs B0740–28 and J2124–3358) are yet to be observed at high angular resolution by *Chandra*. Radio searches to some of these sources have also not been successful at detecting extended emission (Gaensler et al., 2000; Chatterjee and Cordes, 2002). The lack of emission from the termination shock in systems for which the wind is known to be strongly confined is puzzling.

## 6 Conclusions

A consistent understanding is now beginning to emerge of the various multi-wavelength structures seen around high velocity pulsars. As expected, we see

---

<sup>1</sup> This source is one of several nearby isolated neutron stars seen in thermal X-rays, and does not pulse. We assume that this source is a typical pulsar but beaming away from us. To the best of our knowledge, the lack of extended X-ray emission has not been stated in the literature, but is immediately apparent from inspection of deep archival *Chandra* observations of this field.

optical emission from the shocked ISM in several bow shocks, from which we can infer the density of the ambient medium or the Mach number of the system. The morphologies of these shocks also allow us to probe anisotropies in the ISM and in the pulsar wind.

The X-ray and radio emission produced at the termination shock in these systems permit a study of the relativistic wind which drives the bow shock. Just as in the Crab Nebula, high-resolution X-ray imaging allows us to identify both the surface of the termination shock and emission from the post-shock flow. As in the Crab, the effects of an ion-loaded wind and of Doppler beaming are required to explain the observations, suggesting that the wind composition and behaviour is similar for bow shocks and for Crab-like systems. However, a distinct difference from the Crab is the presence of two flow zones downstream, corresponding to highly- and weakly-magnetized material, emerging from the front and back of the termination shock, respectively.

In the near future, we expect that deeper X-ray and optical images will increase the sample and show new types of structure (e.g., Caraveo et al., 2003), and that relativistic magnetohydrodynamical simulations can begin to provide a solid theoretical underpinning for the observed morphologies. The time domain is now also beginning to play a role, in that we can watch bow shocks evolve as they trace the cascade of density inhomogeneities in the ISM (Chatterjee and Cordes, 2004). Clearly bow shocks are now beginning to fulfil their long-standing promise to act as unique probes of pulsars and their surroundings.

## Acknowledgments

I thank all my collaborators with whom I've studied pulsar bow shocks over the last few years. This work has been supported by NASA through SAO grant GO2-3075X and LTSA grant NAG5-13032.

## References

- Aldcroft, T. L., Romani, R. W., Cordes, J. M., 1992. Spectroscopy of the companion and bow-shock nebula of PSR 1957+20. *ApJ* 400, 638–646.
- Arzoumanian, Z., Chernoff, D. F., Cordes, J. M., 2002. The velocity distribution of isolated radio pulsars. *ApJ* 568, 289–301.
- Bucciantini, N., 2002a. Pulsar bow-shock nebulae. II. Hydrodynamical simulation. *A&A* 387, 1066–1073.
- Bucciantini, N., 2002b. Pulsar bow-shock nebulae. III. Inclusion of a neutral component, and  $H\alpha$  luminosity. *A&A* 393, 629–635.

- Camilo, F., Manchester, R. N., Gaensler, B. M., Lorimer, D. R., 2002. Heart-beat of the Mouse: A young radio pulsar associated with the axisymmetric nebula G359.23–0.82. *ApJ* 579, L25–L28.
- Caraveo, P. A., Bignami, G. F., DeLuca, A., Mereghetti, S., Pellizzoni, A., Mignani, R., Tur, A., Becker, W., 2003. Geminga’s tails: A pulsar bow shock probing the interstellar medium. *Science* 301, 1345–1347.
- Chatterjee, S., Cordes, J. M., 2004. Smashing the Guitar: An evolving neutron star bow shock. *ApJ* 600, L51–L54.
- Chatterjee, S., Cordes, J. M., Vlemmings, W. H. T., Arzoumanian, Z., Goss, W. M., Lazio, T. J. W., 2004. Pulsar parallaxes at 5 GHz with the Very Long Baseline Array. *ApJ* 604, 339–345.
- Chatterjee, S., Cordes, J. M., 2002. Bow shocks from neutron stars: Scaling laws and *HST* observations of the Guitar nebula. *ApJ* 575, 407–418.
- Chen, Y., Bandiera, R., Wang, Z.-R., 1996. Approximate analytical expressions of the wind-driven bow shock. *ApJ* 469, 715–718.
- Cordes, J. M., 1996. Pulsar wind nebulae. In: Johnston, S., Walker, M. A., Bailes, M. (Eds.), *Pulsars: Problems and Progress*, IAU Colloquium 160. Astronomical Society of the Pacific, San Francisco, pp. 393–399.
- Cordes, J. M., Lazio, T. J. W., 2002. NE2001. I. A new model for the Galactic distribution of free electrons and its fluctuations. Preprint (astro-ph/0207156).
- Gaensler, B. M., 2004. Shocks and wind bubbles around energetic pulsars. In: Camilo, F., Gaensler, B. M. (Eds.), *Young Neutron Stars and their Environments*. Astronomical Society of the Pacific, San Francisco, pp. 151–158.
- Gaensler, B. M., Jones, D. H., Stappers, B. W., 2002. An optical bow shock around the nearby millisecond pulsar J2124–3358. *ApJ* 580, L137–L141.
- Gaensler, B. M., Stappers, B. W., Frail, D. A., Moffett, D. A., Johnston, S., Chatterjee, S., 2000. Limits on radio emission from pulsar wind nebulae. *MNRAS* 318, 58–66.
- Gaensler, B. M., van der Swaluw, E., Camilo, F., Kaspi, V. M., Baganoff, F. K., Yusef-Zadeh, F., Manchester, R. N., 2004. The Mouse that soared: High resolution X-ray imaging of the pulsar-powered bow shock G359.23–0.82. *ApJ* 616, 383–402.
- Gallant, Y. A., Arons, J., 1994. Structure of relativistic shocks in pulsar winds: A model of the wisps in the Crab Nebula. *ApJ* 435, 230.
- Gvaramadze, V. V., 2004. On the origin of the system PSR B1757–24 / SNR G5.4–1.2. *A&A* 415, 1073–1078.
- Jones, D. H., Stappers, B. W., Gaensler, B. M., 2002. Discovery of an optical bow-shock around pulsar B0740–28. *A&A* 389, L1–L5.
- Kaper, L., van Loon, J. T., Augusteijn, T., Goudfrooij, P., Patat, F., Waters, L. B. F. M., Zijlstra, A. A., 1997. Discovery of a bow shock around Vela X-1. *ApJ* 475, L37–L40.
- Kaspi, V. M., Gotthelf, E. V., Gaensler, B. M., Lyutikov, M., 2001. X-ray detection of pulsar PSR B1757–24 and its nebular tail. *ApJ* 562, L163–

L166.

- Kaspi, V. M., Roberts, M. S. E., Harding, A. K., 2005. Isolated neutron stars. In: Lewin, W. H. G., van der Klis, M. (Eds.), *Compact Stellar X-ray Sources*. CUP, Cambridge, in press (astro-ph/0402136).
- Mann, E. C., Romani, R. W., Fruchter, A. S., 1999. Fabry-Perot imaging of the nearest millisecond pulsar bow-shock. *BAAS* 195, 41.01.
- Moon, D.-S., Lee, J.-J., Eikenberry, S. S., Koo, B.-C., Chatterjee, S., Kaplan, D. L., Hester, J. J., Cordes, J. M., Gallant, Y. A., Koch-Miramond, L., 2004. PSR B1951+32: A bow shock-confined X-ray nebula, a synchrotron knot, and an optical counterpart candidate. *ApJ* 610, L33–L36.
- Ng, C.-Y., Romani, R. W., 2004. Fitting pulsar wind tori. *ApJ* 601, 479–484.
- Olbert, C. M., Clearfield, C. R., Williams, N. E., Keohane, J. W., Frail, D. A., 2001. A bow shock nebula around a compact X-ray source in the supernova remnant IC 443. *ApJ* 554, L205–L208.
- Petre, R., Kuntz, K. D., Shelton, R. L., 2002. The X-ray structure and spectrum of the pulsar wind nebula surrounding PSR B1853+01 in W44. *ApJ* 579, 404–410.
- Stappers, B. W., Gaensler, B. M., Kaspi, V. M., van der Klis, M., Lewin, W. H. G., 2003. An X-ray nebula associated with the millisecond pulsar B1957+20. *Science* 299, 1372–1374.
- Sutherland, R. S., Dopita, M. A., 1995. Young oxygen-rich supernova remnants. II. An oxygen-rich emission mechanism. *ApJ* 439, 381–398.
- van Buren, D., McCray, R., 1988. Bow shocks and bubbles are seen around hot stars by *IRAS*. *ApJ* 329, L93–L96.
- van der Swaluw, E., Achterberg, A., Gallant, Y. A., Downes, T. P., Keppens, R., 2003. Interaction of high-velocity pulsars with supernova remnant shells. *A&A* 397, 913–920.
- van Kerkwijk, M. H., Kulkarni, S. R., 2001. An unusual H-alpha nebula around the nearby neutron star RX J1856.5–3754. *A&A* 380, 221–237.
- Wang, Q. D., Gotthelf, E. V., 1998. *ROSAT* and *ASCA* observations of the Crab-like supernova remnant N157B in the Large Magellanic Cloud. *ApJ* 494, 623.
- Wilkin, F. P., 1996. Exact analytic solutions for stellar wind bow shocks. *ApJ* 459, L31–L34.
- Wilkin, F. P., 2000. Modeling nonaxisymmetric bow shocks: Solution method and exact analytic solutions. *ApJ* 532, 400–414.
- Wong, D. S., Cordes, J. M., Chatterjee, S., Zweibel, E. G., Finley, J. P., Romani, R. W., Ulmer, M. P., 2003. Chandra observations of the Guitar Nebula. In: Li, X. D., Trimble, V., Wang, Z. R. (Eds.), *IAU Symposium 214: High Energy Processes and Phenomena in Astrophysics*. pp. 135–136.
- Zank, G. P., 1999. Interaction of the solar wind with the local interstellar medium: A theoretical perspective. *Space Sci. Rev.* 89, 413–688.
- Zavlin, V. E., Pavlov, G. G., Sanwal, D., Manchester, R. N., Trümper, J., Halpern, J. P., Becker, W., 2002. X-radiation from the millisecond pulsar J0437–4715. *ApJ* 569, 894–902.

This figure "fig1.gif" is available in "gif" format from:

<http://arxiv.org/ps/astro-ph/0501357v1>